Heterometallic Complexes

International Edition: DOI: 10.1002/anie.201803761
German Edition: DOI: 10.1002/ange.201803761

Structure and Magnetization Dynamics of Dy–Fe and Dy–Ru Bonded Complexes

*Corey P. Burns, Xin Yang, Joshua D. Wofford, Nattamai S. Bhuvanesh, Michael B. Hall, and Michael Nippe**

Abstract: *We present an investigation of isostructural complexes that feature unsupported direct bonds between a formally trivalent lanthanide ion (Dy^{3+}) and either a first-row (Fe) or a second-row (Ru) transition metal (TM) ion. The sterically rigid, yet not too bulky ligand $PyCp_2^{2-}$ ($PyCp_2^{2-}$ = [2,6-$(CH_2C_5H_3)_2C_5H_3N]^{2-}$) facilitates the isolation and characterization of $PyCp_2Dy{-}FeCp(CO)_2$ (**1**; d(Dy–Fe) = 2.884(2) Å) and $PyCp_2Dy{-}RuCp(CO)_2$ (**2**; d(Dy–Ru) = 2.9508(5) Å). Computational and spectroscopic studies suggest strong TM→Dy bonding interactions. Both complexes exhibit field-induced slow magnetic relaxation with effectively identical energy barriers to magnetization reversal. However, in going from Dy–Fe to Dy–Ru bonding, we observed faster magnetic relaxation at a given temperature and larger direct and Raman coefficients, which could be due to differences in the bonding and/or spin–phonon coupling contributions to magnetic relaxation.*

Direct unsupported bonds between lanthanide (Ln) and transition metal (TM) ions are among the least well understood classes of interatomic interactions in chemistry.[1] This is largely due to the significant synthetic challenges associated with isolating discrete Ln–TM bonded complexes, specifically those that feature unsupported Ln–TM bonds. The first report of a structurally characterized direct lanthanide–transition metal bond in $(thf)Cp_2Lu{-}RuCp(CO)_2$ (Cp = $C_5H_5^-$) by Beletskaya[2] and co-workers suggested that anionic TM complexes with charge localized at the TM ion (such as in $[FeCp(CO)_2]^-$ and $[RuCp(CO)_2]^-$) should be valuable synthons for the generation of Ln–TM bonds by salt elimination reactions. This approach has also proven successful for the isolation of a thermally stable Nd–Fe bonded complex.[3] A powerful alternative method for the generation of discrete Ln–TM bonded molecular species was introduced in 2008 by Kempe and co-workers, who established the versatile utility of alkane elimination reactions between Ln–alkyl and acidic TM–hydride species.[4a] This method was also exploited to generate a Lu–Re bonded species,[4b] and was further shown to enable the formation of remarkable complexes that feature three intramolecular Ln–Re bonds (Ln = Sm, Lu, La).[4c]

However, even given these important and elegant discoveries, there are still no synthetic procedures that would allow altering the nature of both the TM and the Ln ion systematically in an isostructural family of Ln–TM bonded complexes. These systems would be important contributions towards a physical description of the nature of Ln–TM bonding. There is currently an ongoing debate about the degree of covalency in metal–ligand bonding of the f block elements, and recent experimental results are reshaping our understanding of how f block elements interact with ligands.[5]

In addition to answering fundamental questions about bonding, we are particularly interested in studying Ln–TM bonded complexes with respect to their static and dynamic magnetic properties. Specifically, the large single-ion anisotropy of trivalent Ln ions, such as Dy^{3+} [6] and Tb^{3+},[7] renders them promising candidates for the field of single molecule magnets (SMMs).[8] Whereas SMM behavior has been reported for Ln–main group metal SMMs,[9] to the best of our knowledge, no magnetization dynamics have been reported for any Ln–TM bonded complexes.

Herein, we present the first structural, spectroscopic, magnetic, and computational comparison of Ln–Fe and Ln–Ru bonding (Ln = Dy) in discrete molecules.

The judicious choice of lanthanide starting materials is crucial if Ln–TM bonds are to be generated. If species such as $[FeCp(CO)_2]^-$ are to be used, the Ln–TM bond has to outcompete the oxophilicity of the Ln ion, which would favor the formation of Ln isocarbonyl complexes. Similarly, the steric bulk of the Ln-supporting ligand has to be minimized to avoid the formation of isocarbonyl species. For example, the steric bulk around the Dy^{3+} ion in its bis(pentamethylcyclopentadienyl) complexes favors the formation of isocarbonyl complexes over the formation of Dy–Fe bonds in reactions between $Cp^*_2Dy(PhBPh_3)$ and $[FeCp(CO)_2]^-$.[10] As such, we can formulate two prerequisites for the formation of Ln–TM bonds: 1) The Ln ions need to be sterically accessible, and 2) the metal-centered charge needs to be localized on the TM fragment in such a way as to favor Ln–TM over Ln–OC–TM bonding. We identified the structurally rigid yet not overly sterically demanding ligand $PyCp_2^{2-}$ ($PyCp_2^{2-}$ = [2,6-$(CH_2C_5H_3)_2C_5H_3N]^{2-}$)[11] as a potential ligand platform for the generation of Ln–TM bonded species. The triflate-bridged dinuclear Dy^{3+} complex shown in Scheme 1 dissociates readily in thf solution into its corresponding monomers,[11c] which can be reacted with stoichiometric amounts of $K[FeCp(CO)_2]$ or $K[RuCp(CO)_2]$ to yield crystalline material

[*] C. P. Burns, X. Yang, J. D. Wofford, Dr. N. S. Bhuvanesh, Prof. M. B. Hall, Prof. M. Nippe
Department of Chemistry, Texas A&M University
3255 TAMU, College Station, TX 77843 (USA)
E-mail: nippe@chem.tamu.edu

Supporting information and the ORCID identification number(s) for the author(s) of this article can be found under: https://doi.org/10.1002/anie.201803761.

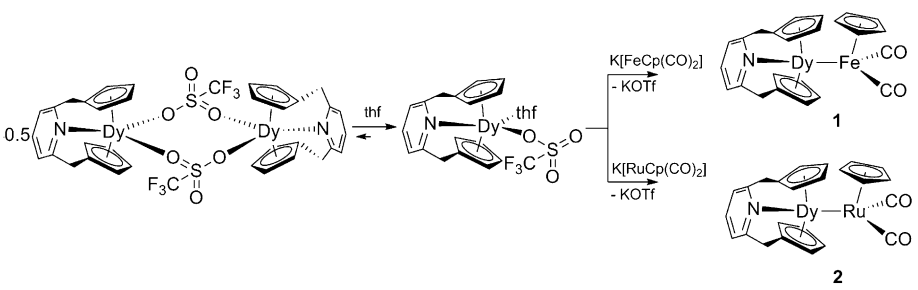

Scheme 1. Synthesis of **1** and **2**.

of $PyCp_2Dy$-$FeCp(CO)_2$ (**1**) and $PyCp_2Dy$-$RuCp(CO)_2$ (**2**), respectively.

The molecular structures of **1** and **2** (Figure 1; see also Tables S1 and S2) feature Dy–Fe and Dy–Ru distances of 2.884(2) Å and 2.951(1) Å. To the best of our knowledge, these are the first direct unsupported Dy–TM bonds reported

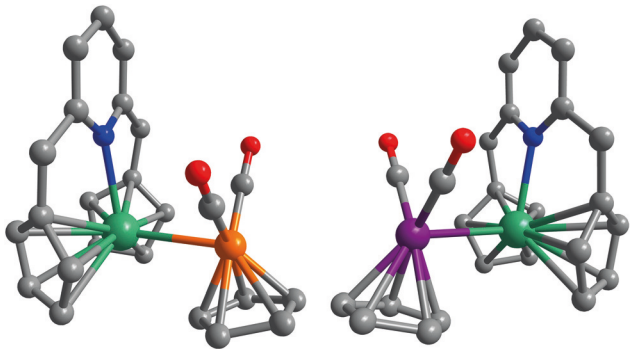

Figure 1. Molecular structure of **1** (left) and **2** (right).[28] Hydrogen atoms have been omitted for clarity. Dy green, Ru purple, Fe orange, N blue, O red, C gray.

thus far. It is interesting to note that the Dy–Ru bond in **2** is approximately 0.03 Å longer than the Dy–Ru distances in a reported hydride-bridged species.[12] All other Dy–ligand distances in **1** and **2** are statistically the same (d(Dy–N) = 2.452(9) Å and 2.470(3) Å; d(Dy–C) = 2.628[7] Å and 2.631-[3] Å). The spectroscopic features of the new Dy–TM bonded species are particularly interesting. The ^{57}Fe Mössbauer spectra of **1** (see the Supporting Information, Figure S1) obtained at 5 K (or 120 K) feature a single doublet with an isomer shift (δ) of 0.129 mm s^{-1} (or 0.116 mm s^{-1}) and a quadrupole splitting (ΔE_Q) of 1.859 mm s^{-1} (or 1.862 mm s^{-1}). The isomer shift reflects the s electron density at the iron nucleus (δ decreases with increasing s electron density) as well as the p/d electron density, which shields the s electron density (δ increases with increasing ligand-to-Fe π donation).[13a] The values obtained for **1** occupy a somewhat unique niche for $Cp(CO)_2Fe$–X complexes. The δ value of **1** is larger than those of formally Fe^{2+} $Cp(CO)_2Fe$–X species in which X is not a π-donor ligand (X = CN/CH_3: δ = 0.069/0.069 mm s^{-1}; ΔE_Q = 1.899/1.746 mm s^{-1} at 78 K)[13a,b] as well as in formally Fe^0 $Cp(CO)_2Fe$–X species (X = LGe^{4+} (at 78 K)/LFe^{2+} (at 190 K): δ = 0.084/0.080 mm s^{-1}; ΔE_Q = 1.74/1.73 mm s^{-1}).[13c,e] However, the δ value measured for **1** is lower than in formally Fe^{2+} $Cp(CO)_2Fe$–X complexes where X is a σ- and a π-donor ligand (X = NCS/I: (δ = 0.202/0.215 mm s^{-1}; ΔE_Q = 1.878/1.840 mm s^{-1} at 78 K).[13a] In the case of **1**, the isomer shift is likely solely dominated by the s electron density at Fe, which is a function of the strength of the Fe→Dy σ donation. Based on these considerations, one tentative interpretation of the data is that complex **1** contains a formally Fe^0 species and stronger Fe→X σ donation (X = Dy^{3+}) than Fe–Ge and Fe–Fe bonded species, which results in a higher δ value. This interpretation was further supported by IR spectroscopy. The energies associated with the CO stretching modes in **1** (1910, 1840 cm^{-1}) and **2** (1930, 1851 cm^{-1}) are rather similar to those reported for other formally Fe^0 species, such as Cu–Fe (1914, 1849 cm^{-1}) and Zn–Fe bonded complexes (1944, 1888 cm^{-1}),[13d] and much lower than those for $Cp(CO)_2Fe$–I (2038, 1988 cm^{-1}).

There is precedence for utilizing the QTAIM model[14] to describe aspects of heterometallic interactions in Ln–TM bonded complexes computationally.[15] Accordingly, we used DFT calculations to obtain relevant parameters. Our analysis was carried out using the Gaussian09[16] (BP86;[17] Dy: cc-pVTZ-DK3 (all electron);[18] Ru[19] or Fe:[20] cc-pVTZ-DK (all electron); 6–311G(d))[21] and ADF[22] (BP86; TZ2P; ZORA) software packages. Both packages were used for calculations on the experimentally observed molecular geometries of **1** and **2** from single-crystal X-ray diffraction, and the geometries were optimized with the ADF package (Table S3). In all cases, we observed critical points along the lines between Dy and Fe or Dy and Ru (LCPs; Figure 2). For **1**, these LCPs are found at the very center of the Dy–Fe bond (d(Dy–LCP) = d(Fe–LCP) = 1.44 Å) while for **2**, the LCPs are closer to the Dy than to the Ru ion (d(Dy–LCP): 1.41 Å; d(Ru–LCP) = 1.54 Å). Interestingly, when the experimental crystal structure was used, the delocalization index (DI-G09 or DI-ADF) was slightly larger for Dy–Fe (0.45 or 0.44) than for Dy–Ru (0.43 or 0.42) while the reverse was true for geometry-optimized structures (DI(Dy,Fe) = 0.47; DI(Dy,Ru) = 0.48). Although the differences in the calculated DIs are admittedly small, larger DIs for the Dy–Fe as compared to the Dy–Ru bonded system would indicate increased electron sharing between Dy and the first-row transition metal Fe as compared to its heavier congener Ru. This surprising finding appears to be further supported by consistently larger positive Laplacians of the electron density at the LCPs ($\nabla^2\rho$(LCP)) for Dy–Ru than for Dy–Fe. As has been pointed out,[23] care must be taken in interpreting these QTAIM results, and no direct translation of them into a chemist's interpretation of bond, bonding, or bond strength is obvious. However, these results do support a model in which more direct interactions occur between Dy and Fe than between Dy and Ru. Qualitatively, these findings are in line with the significantly greater nucleophilicity of $[FeCp(CO)_2]^-$ as compared to that of $[RuCp(CO)_2]^-$,[24] and may be interpreted as a result of the stronger ruthenium–ligand interactions (as compared to iron–

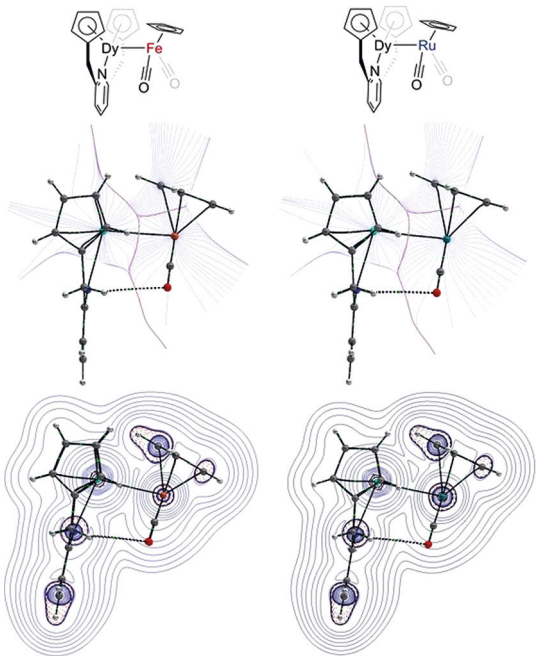

Figure 2. Basin paths with interatomic surface paths (center) and contour plots of $\nabla^2\rho$ (bottom) for **1** (left) and **2** (right).

ligand interactions), which attenuate the contribution of the Ru-centered anionic charge to the electrostatic stabilizing interaction of the polar, yet not purely ionic, Dy–Ru bond.

The static magnetic properties of **1** and **2** were probed by variable-temperature direct current (dc) magnetometry using a 1000 Oe applied field (Figures S2 and S3). The room-temperature $\chi_M T$ values of 13.75 and 13.56 emu K mol^{-1} for **1** and **2**, respectively, are close to, but somewhat lower than, the expected value of 14.17 emu K mol^{-1} for a mononuclear Dy^{3+} complex ($^6H_{15/2}$, $S=5/2$, $L=5$, $g=4/3$). Such small deviations from the expected value are frequently observed for mononuclear Dy^{3+} complexes. As such, a formal ion charge assignment of Dy^{3+}–Fe^0 would still be consistent with the magnetic data, but partial electron donation from Fe to Dy seems also possible. Both complexes exhibit a gradual decrease in their respective $\chi_M T$ values upon lowering the temperature. This decrease in $\chi_M T$ is typically observed and attributed to the depopulation of Stark sublevels of Dy^{3+}. Both **1** and **2** display a slight increase in $\chi_M T$ at the lowest temperatures (2 K), which could be indicative of weak intermolecular ferromagnetic interactions. Variable-temperature magnetization versus field measurements for **1** and **2** (Figures S4 and S6) indicate that both complexes do not reach magnetic saturation up to a field of 7 T with significantly smaller magnetization values (4.73 μ_B (for **1**) and 4.87 μ_B (for **2**) at 1.8 K and 7 T) than the expected free ion value (10 μ_B for a Dy^{3+} ion). This discrepancy suggests breaking of the degeneracy of the $^6H_{15/2}$ ground state by crystal/ligand field effects.[25] The M versus H/T curves for **1** and **2** (Figures S5 and S7) are non-superimposable due to the magnetically highly anisotropic Dy^{3+} ions.

The dynamic magnetic properties of **1** and **2** were probed by variable-temperature alternating current (ac) magnetometry. In the absence of an externally applied dc field, no signals in the out-of-phase component of the ac susceptibility (χ_M'') could be observed in the temperature range of 2–10 K. This is likely a result of quantum tunneling of the magnetization (QTM). Application of dc fields proved successful in significantly reducing QTM processes in **1** and **2** and allowed for the observation of χ_M'' signals. The dc field dependence of the ac signals at 4 K (Figures S8 and S9), the corresponding Cole–Cole plots (Figures S10 and S11), and relaxation times (τ; obtained from fitting Cole–Cole plots to the generalized Debye equation; Figures S12 and S13) as a function of the dc field for **1** and **2** are provided in the Supporting Information. Both complexes show an initial increase in τ with increasing dc fields, which is due to the decreasing contribution of QTM to the magnetic relaxation rates. Optimal dc fields of 1500 Oe (for **1**) and 1600 Oe (for **2**) were observed. The application of larger dc fields induces a direct process to occur and accelerates magnetic relaxation, as can be seen in the decrease in the τ values at fields larger than 1500 Oe (for **1**) and 1600 Oe (for **2**). It is interesting to note that under comparable fields, complex **1** always exhibits significantly larger τ values than **2**. The field dependence of τ at 4 K was fit according to $\tau^{-1} = AH^{n_1}T + B_1/(1+B_2H^2) + D$; here, A is the direct relaxation parameter, B_1 and B_2 are QTM parameters, and D accounts for field-independent contributions from Raman and Orbach processes.[26] Constraining n_1 to a value of 4[8c] and letting all other values refine freely, we obtained the values shown in Table S4. Variable-temperature ac measurements were performed at the optimized dc fields. Figure 3 shows the χ_M'' signals observed for **1** and **2** (see Figures S13 and S14 for χ_M' data). These data were used to construct

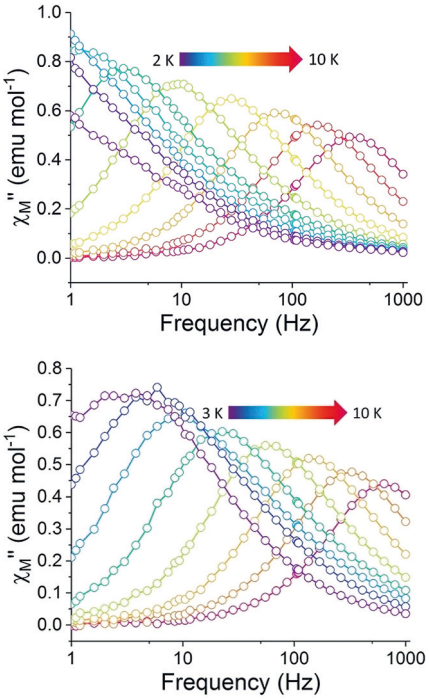

Figure 3. Frequency dependence of the out-of-phase (χ_M'') component of the molar ac susceptibility of **1** (at an applied dc field of 1500 Oe, top) and **2** (at an applied dc field of 1600 Oe, bottom).

Cole–Cole plots (Figure S15 and S16), from which relaxation times were extracted, which were used to obtain Arrhenius plots.

There are several approaches to estimating the effective energy barrier to magnetization reversal (U_{eff}) from Arrhenius plots. Fitting solely the linear region of the Arrhenius plots according to $\tau^{-1} = \tau_0{}^{-1} \times e^{-U_{eff}/k_B T}$ (Figures S17 and S18) yielded U_{eff} (and τ_0) values of 40 cm^{-1} (and 1.5×10^{-6} s) and 36 cm^{-1} (and 1.41×10^{-6} s) for **1** and **2**, respectively. The similarity of the U_{eff} values for **1** and **2** is very interesting and suggests that the energy of the relaxation-relevant (likely first) excited m_J states is not strongly altered in going from a Dy–Fe bond in **1** to a Dy–Ru bond in **2**, even though the relaxation times at a given field and temperature are always longer for **1** than for **2**. Similar results were obtained by fitting the whole temperature region of the Arrhenius plots according to $\tau^{-1} = AH^4T + \tau_{QTM}{}^{-1} + CT^{n_2} + \tau_0{}^{-1}e^{-U_{eff}/k_B T}$. Here, we restricted n_2 to a value of 5[8c] and fixed the parameters A, B_1, and B_2 to those obtained above from the variable dc field dependence of τ to avoid over-parameterization. The best fits (Figure 4) resulted in extracted U_{eff} (and τ_0) values of 43 cm^{-1}

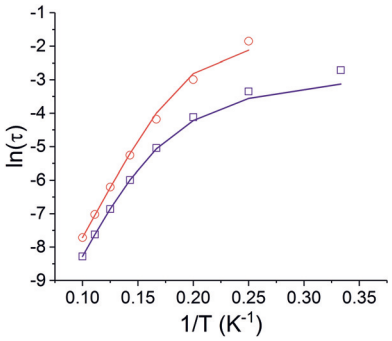

Figure 4. Arrhenius plots for **1** (red circles) and **2** (purple squares) at 1500 Oe and 1600 Oe, respectively. Lines correspond to the fit described in the text.

(and 1.0×10^{-6} s) and 46 cm^{-1} (and 5.4×10^{-7} s) for **1** and **2**, respectively. Of course, mathematically better fits can be obtained by refining all components of the equation, but we preferred to not over-parameterize the fitting routine. However, it appears clear that independent of the fitting method, **1** and **2** display surprisingly similar, if not identical, U_{eff} values.

In summary, we have presented the first structural, computational, and magnetic comparison of isostructural Dy complexes that feature a Dy ion bound directly to either a first-row or a second-row transition-metal ion. Spectroscopic and computational analysis suggested strong TM→Dy σ donation. The barriers to magnetization reversal are effectively identical for **1** and **2** whereas the optimal dc fields are different, and, importantly, magnetic relaxation is slower for **1** than for **2** at a given temperature, and **2** displays larger coefficients for direct and Raman processes. These observations are likely to be consequences of subtle changes in the nature of the Ln–TM bonding as well as changes of the effect of spin–phonon coupling on magnetic relaxation,[8c,27] as the energies of all TM–ligand vibrational modes, and especially those of the Dy–TM one, will be strongly altered upon going from **1** to **2**. The herein reported powerful synthetic approach should also enable studies of a wide variety of Ln–TM bonded complexes in a systematic fashion. This work is currently ongoing in our laboratories.

Acknowledgements

M.N. is grateful for financial support by The Welch Foundation (A-1880). M.B.H. thanks the National Science Foundation (Grant No. CHE-1664866) and The Welch Foundation (Grant No. A-0648) for support of this work. We thank B. Foley, A. Kosanovich, and O. Ozerov for their help in obtaining IR spectra. ^{57}Fe Mössbauer spectra were acquired on instruments housed in the Dr. P. A. Lindahl research group (NIH, GM084266).

Conflict of interest

The authors declare no conflict of interest.

Keywords: dysprosium · heterometallic complexes · lanthanide–transition metal bonding · magnetic properties · organometallic chemistry

How to cite: *Angew. Chem. Int. Ed.* **2018**, *57*, 8144–8148
Angew. Chem. **2018**, *130*, 8276–8280

[1] M. V. Butovskii, R. Kempe, *New J. Chem.* **2015**, *39*, 7544.
[2] a) G. K.-I. Magomedov, A. Z. Voskoboynikov, E. B. Chuklanova, A. I. Gusev, I. P. Beletskaya, *Organomet. Chem. (USSR)* **1990**, *3*, 360; b) I. P. Beletskaya, A. Z. Voskoboynikov, E. B. Chuklanova, N. I. Kirillova, A. K. Shestakova, I. N. Parshina, A. I. Gusev, G. K.-I. Magomedov, *J. Am. Chem. Soc.* **1993**, *115*, 3156.
[3] P. L. Arnold, J. McMaster, S. T. Liddle, *Chem. Commun.* **2009**, 818.
[4] a) M. V. Butovskii, O. L. Tok, F. R. Wagner, R. Kempe, *Angew. Chem. Int. Ed.* **2008**, *47*, 6469; *Angew. Chem.* **2008**, *120*, 6569; b) M. V. Butovskii, O. L. Tok, V. Bezugly, F. R. Wagner, R. Kempe, *Angew. Chem. Int. Ed.* **2011**, *50*, 7695; *Angew. Chem.* **2011**, *123*, 7837; c) M. V. Butovskii, C. Döring, V. Bezugly, F. R. Wagner, Y. Grin, R. Kempe, *Nat. Chem.* **2010**, *2*, 741.
[5] a) M. W. Löble, J. M. Keith, A. B. Altman, S. C. E. Stieber, E. R. Batista, K. S. Boland, S. D. Conradson, D. L. Clark, J. Lezama Pacheo, S. A. Kozimor, R. L. Martin, S. G. Minasian, A. C. Olson, B. L. Scott, D. K. Shuh, T. Tyliszak, M. P. Wilkerson, R. A. Zehnder, *J. Am. Chem. Soc.* **2015**, *137*, 2506; b) J. N. Cross, J. Su, E. R. Batista, S. K. Cary, W. J. Evans, S. A. Kozimor, V. Mocko, B. L. Scott, B. W. Stein, C. J. Windorff, P. Yang, *J. Am. Chem. Soc.* **2017**, *139*, 8667; c) S. G. Minasian, E. R. Batista, C. H. Booth, D. L. Clark, J. M. Keith, S. A. Kozimor, W. W. Lukens, R. L. Martin, D. K. Shuh, S. C. E. Stieber, T. Tylisczcak, X.-d. Wen, *J. Am. Chem. Soc.* **2017**, *139*, 18052.
[6] a) C. A. P. Goodwin, F. Ortu, D. Reta, N. F. Chilton, D. P. Mills, *Nature* **2017**, *548*, 439; b) F.-S. Guo, B. M. Day, Y.-C. Chen, M.-L. Tong, A. Mansikkamäki, R. A. Layfield, *Angew. Chem. Int. Ed.* **2017**, *56*, 11445; *Angew. Chem.* **2017**, *129*, 11603; c) J. Liu, Y.-C. Chen, J.-L. Liu, V. Vieru, L. Ungur, J.-H. Jia, L. F. Chibotaru, Y. Lan, W. Wernsdorfer, S. Gao, X.-M. Chen, M.-L. Tong, *J. Am. Chem. Soc.* **2016**, *138*, 5441; d) Y.-C. Chen, J.-L. Liu, L. Ungur, J.

Liu, Q.-W. Li, L.-F. Wang, Z.-P. Ni, L. F. Chibotaru, X.-M. Chen, M.-L. Tong, *J. Am. Chem. Soc.* **2016**, *138*, 2829; e) S. K. Gupta, T. Rajeshkumar, G. Rajaraman, R. Murugave, *Chem. Sci.* **2016**, *7*, 5181; f) L. Norel, L. E. Darago, B. L. Guennic, K. Chakarawet, M. I. Gonzalez, J. H. Olshansky, S. Rigaut, J. R. Long, *Angew. Chem. Int. Ed.* **2018**, *57*, 1933; *Angew. Chem.* **2018**, *130*, 1951.

[7] a) N. Ishikawa, M. Sugita, T. Ishikawa, S. Koshihara, Y. Kaizu, *J. Am. Chem. Soc.* **2003**, *125*, 8694; b) S. Takamatsu, T. Ishikawa, S.-y. Koshihara, N. Ishikawa, *Inorg. Chem.* **2007**, *46*, 7250.

[8] a) D. N. Woodruff, R. E. P. Winpenny, R. A. Layfield, *Chem. Rev.* **2013**, *113*, 5110; b) R. A. Layfield, *Organometallics* **2014**, *33*, 1084; c) J. van Slageren, S. T. Liddle, *Chem. Soc. Rev.* **2015**, *44*, 6655; d) J. Lu, M. Guo, J. Tang, *Chem. Asian J.* **2017**, *12*, 2772; e) J. D. Rinehart, J. R. Long, *Chem. Sci.* **2011**, *2*, 2078.

[9] T. Pugh, N. F. Chilton, R. A. Layfield, *Chem. Sci.* **2017**, *8*, 2073.

[10] T. Pugh, N. F. Chilton, R. A. Layfield, *Angew. Chem. Int. Ed.* **2016**, *55*, 11082; *Angew. Chem.* **2016**, *128*, 11248.

[11] a) G. Paolucci, R. D'Ippolito, C. Ye, C. Qian, J. Gräper, R. D. Fischer, *J. Organomet. Chem.* **1994**, *471*, 97; b) G. Paolucci, J. Zanon, V. Lucchini, W.-E. Damrau, D. E. Siebel, R. D. Fischer, *Organometallics* **2002**, *21*, 1088; c) C. P. Burns, B. O. Wilkins, C. M. Dickie, T. P. Latendresse, L. Vernier, K. R. Vignesh, N. S. Bhuvanesh, M. Nippe, *Chem. Commun.* **2017**, *53*, 8419.

[12] W. W. N. O, X. Xiaohui Kang, Y. Luo, Z. Hou, *Organometallics* **2014**, *33*, 1030.

[13] a) G. J. Long, D. G. Alway, K. W. Barnett, *Inorg. Chem.* **1978**, *17*, 486; b) H. Nakazawa, S. Ichimura, Y. Nishihara, K. Miyoshi, S. Nakashima, H. Sakai, *Organometallics* **1998**, *17*, 5061; c) N. Kano, N. Yoshinari, Y. Shibata, M. Miyachi, T. Kawashima, M. Enomoto, A. Okazawa, N. Kojima, J.-D. Guo, S. Nagase, *Organometallics* **2012**, *31*, 8059; d) M. K. Karunananda, F. X. Vázquez, E. E. Alp, W. Wenli Bi, S. Chattopadhyay, T. Shibatad, N. P. Mankad, *Dalton Trans.* **2014**, *43*, 13661; e) H. Lei, J.-D. Guo, J. C. Fettinger, S. Nagase, P. P. Power, *J. Am. Chem. Soc.* **2010**, *132*, 17399.

[14] R. F. W. Bader, *Atoms in Molecules: A Quantum Theory*, Clarendon Press, Oxford, **1990**, p. xviii, p. 438.

[15] a) B. Vlaisavljevich, P. Miró, C. J. Cramer, L. Gagliardi, I. Infante, S. T. Liddle, *Chem. Eur. J.* **2011**, *17*, 8424; b) M. V. Butovskii, B. Oelkers, T. Bauer, J. M. Bakker, V. Bezugly, F. R. Wagner, R. Kempe, *Chem. Eur. J.* **2014**, *20*, 2804.

[16] Gaussian 09, Revision D.01, M. J. Frisch et al., Gaussian, Inc.: Wallingford CT, **2009**.

[17] a) A. D. Becke, *Phys. Rev. A* **1988**, *38*, 3098; b) J. P. Perdew, *Phys. Rev. B* **1986**, *33*, 8822.

[18] Q. Lu, K. A. Peterson, *J. Chem. Phys.* **2016**, *145*, 054111.

[19] K. A. Peterson, D. Figgen, M. Dolg, H. Stoll, *J. Chem. Phys.* **2007**, *126*, 124101.

[20] N. Balabanov, K. A. Peterson, *J. Chem. Phys.* **2005**, *123*, 064107.

[21] R. J. Krishnan, S. Binkley, R. Seeger, J. A. Pople, *J. Chem. Phys.* **1980**, *72*, 650.

[22] a) G. te Velde, F. M. Bickelhaupt, E. J. Baerends, C. Fonseca Guerra, S. J. A. van Gisbergen, J. G. Snijders, T. Ziegler, *J. Comput. Chem.* **2001**, *22*, 931; b) C. Fonseca Guerra, J. G. Snijders, G. te Velde, E. J. Baerends, *Theor. Chem. Acc.* **1998**, *99*, 391; c) ADF2017, SCM, Theoretical Chemistry, Vrije Universiteit, Amsterdam, The Netherlands, http://www.scm.com.

[23] a) C. Foroutan-Nejad, S. Shahbazian, R. Marek, *Chem. Eur. J.* **2014**, *20*, 10140; b) S. Shahbazian, *Chem. Eur. J.* **2018**, *24*, 5401 – 5405.

[24] B. B. King, *Acc. Chem. Res.* **1970**, *3*, 417.

[25] R. A. Layfield, J. J. W. McDouall, S. A. Sulway, F. Tuna, D. Collison, R. E. P. Winpenny, *Chem. Eur. J.* **2010**, *16*, 4442.

[26] V. V. Novikov, A. A. Pavlov, Y. V. Nelyubina, M.-E. Boulon, O. A. Varzatskii, Y. Z. Voloshin, R. E. P. Winpenny, *J. Am. Chem. Soc.* **2015**, *137*, 9792.

[27] a) A. Lunghi, F. Totti, R. Sessoli, S. Sanvito, *Nat. Commun.* **2017**, *8*, 14620; b) A. Lunghi, F. Totti, S. Sanvito, R. Sessoli, *Chem. Sci.* **2017**, *8*, 6051.

[28] CCDC 1833340 (**1**) and 1833341 (**2**) contain the supplementary crystallographic data for this paper. These data can be obtained free of charge from The Cambridge Crystallographic Data Centre.

Manuscript received: March 28, 2018
Revised manuscript received: April 28, 2018
Accepted manuscript online: May 2, 2018
Version of record online: May 30, 2018

